Proton Transfer from Asp-96 to the Bacteriorhodopsin Schiff Base Is Caused by a Decrease of the pK_a of Asp-96 Which Follows a Protein Backbone Conformational Change†

Yi Cao,‡ György Váró,§ Alexandra L. Klinger,∥ Daniel M. Czajkowsky,∥ Mark S. Braiman,∥ Richard Needleman,⊥ and Janos K. Lanyi*,‡

Department of Physiology and Biophysics, University of California, Irvine, California 92717, Biological Research Center of the Hungarian Academy of Sciences, H-6701 Szeged, Hungary, Department of Biochemistry, University of Virginia Health Sciences Center, Charlottesville, Virginia 22908, and Department of Biochemistry, Wayne State University School of Medicine, Detroit, Michigan 48201

Received September 16, 1992; Revised Manuscript Received December 9, 1992

ABSTRACT: In the bacteriorhodopsin photocycle the transported proton crosses the major part of the hydrophobic barrier during the M to N reaction; in this step the Schiff base near the middle of the protein is reprotonated from D96 located near the cytoplasmic surface. In the recombinant D212N protein at pH >6, the Schiff base remains protonated throughout the photocycle [Needleman, Chang, Ni, Váró, Fornés, White, & Lanyi (1991) *J. Biol. Chem. 266,* 11478–11484]. Time-resolved difference spectra in the visible and infrared are described by the kinetic scheme BR $\xrightarrow{h\nu}$ K ↔ L ↔ N (→N′) → BR. As evidenced by the large negative 1742-cm^{-1} band of the COOH group of the carboxylic acid, deprotonation of D96 in the N state takes place in spite of the absence of the unprotonated Schiff base acceptor group of the M intermediate. Instead of internal proton transfer to the Schiff base, the proton is released to the bulk, and can be detected with the indicator dye pyranine during the accumulation of N′. The D212N/D96N protein has a similar photocycle, but no proton is released. As in wild-type, deprotonation of D96 in the N state is accompanied by a protein backbone conformational change indicated by characteristic amide I and II bands. In D212N the residue D96 can thus deprotonate independent of the Schiff base, but perhaps dependent on the detected protein conformational change. This could occur through increased charge interaction between D96 and R227 and/or increased hydration near D96. We suggest that the proton transfer from D96 to the Schiff base in the wild-type photocycle is driven also by such a decrease in the pK_a of D96.

The proton translocation mechanism in bacteriorhodopsin is based on directed sequential changes of the pK_a's of the retinal Schiff base and strategically located aspartate residues in this light-driven pump [reviewed recently in Mathies et al. (1991), Rothschild (1992), Lanyi (1992), and Oesterhelt et al. (1992)]. Isomerization of the retinal around the C_{13}–C_{14} double bond from trans to cis upon illumination is followed by transfer of the Schiff base proton to D85, a residue near the extracellular protein surface. Protonation of D85 triggers the release of a proton, either from R82 or from a group strongly influenced by R82 (Braiman et al., 1988a; Otto et al., 1990; Zimányi et al., 1992b), and the deprotonated Schiff base then changes its access from the extracellular to the cytoplasmic side [the essential switch reaction of the pump (Nagle & Mille, 1981; Schulten et al., 1984; Fodor et al., 1988; Henderson et al., 1990; Váró & Lanyi, 1991a,c)]. Reprotonation of the Schiff base is therefore by D96, a protonated residue near the cytoplasmic surface. Replacement of the proton of D96 from the bulk is concurrent with reisomerization of the retinal, and the initial state is finally regained by transfer of a proton from D85 to the initial proton release group. When the pH is below the pK_a of the proton release group (calculated to be 5.8), the proton pathway is somewhat different: the proton release on the extracellular side is delayed until after proton uptake on the cytoplasmic side, i.e., at the time when D85 deprotonates at the end of the photocycle (Zimányi et al., 1992b). Both of these proton-transfer pathways result in the net translocation of a proton across the protein. The intermediate states in the reaction sequence have distinct spectra in the visible and the infrared, and have been named K, L, M, N, and O (Lozier et al., 1975). The kinetic scheme which describes the photocycle has long been controversial. A considerable body of evidence for various partial reactions of the cycle (Chernavskii et al., 1989; Otto et al., 1989; Váró & Lanyi, 1990a, 1991a,c; Gerwert et al., 1990; Cao et al., 1991; Ames & Mathies, 1990; Milder et al., 1991; Nagle, 1991; Sasaki et al., 1992; Lozier et al., 1992; Zimányi et al., 1992a,b; Druckmann et al., 1992) supports the combined sequence BR $\xrightarrow{h\nu}$ K ↔ L ↔ M_1 → M_2 ↔ M_N ↔ N ↔ O → BR.

The details of the reprotonation of the Schiff base by D96 in the M to N reaction segment are now beginning to become clear. The proton passes through what appears to be a narrow or partly occluded 10-Å-long channel lined with mostly hydrophobic residues (Henderson et al., 1990). Replacing D96 with nonprotonable residues causes considerable slowing of the proton transfer which otherwise takes place in about 3 ms, and makes the reaction dependent on pH (Tittor et al., 1989; Otto et al., 1989; Miller & Oesterhelt, 1990; Cao et al., 1991). Since in the absence of a protonable residue at position 96 the rate-limiting step is thus the capture of a proton on the

† This work was supported by grants from the U.S. Department of Energy (DE-FG03-86ER13525 to J.K.L. and DE-FG02-92ER20089 to R.N.), the National Institutes of Health (GM 29498 to J.K.L. and 5-S07RR0531-30 to M.S.B.), and the Lucille P. Markey Charitable Trust (to M.S.B.).

* To whom correspondence should be addressed.
‡ University of California.
§ Biological Research Center of the Hungarian Academy of Sciences.
∥ University of Virginia Health Sciences Center.
⊥ Wayne State University School of Medicine.

0006-2960/93/0432-1981$04.00/0

protein surface, the reprotonation of the Schiff base is no longer an internal proton transfer as in wild-type. This interpretation is confirmed by the finding that hydrogen azide can function as an external proton donor in this system (Tittor et al., 1989; Otto et al., 1989; Cao et al., 1991), shuttling between the protein interior and the bulk and restoring both fast reprotonation of the Schiff base and transport.

The *rate of proton transfer* from D96 to the deprotonated Schiff base is apparently determined by the high enthalpy of a transition state (Cao et al., 1991) in which the proton occupies an intermediate position between donor and acceptor, i.e., $COO^-..H^+..N$. The main contribution to this barrier is the electrostatic self-energy of the ion pair because replacing D96 with asparagine lowers the enthalpy of activation by 40 kJ/mol. In the wild-type protein, but not in D96N, osmotically active solutes increase the barrier, suggesting that when the proton transfer involves charge separation it is facilitated by water bound inside the protein which stabilizes the transition state.

The *protonation equilibrium* is determined, on the other hand, by the difference in the pK_a's of the Schiff base and D96. In the initial state, both of these pK_a's are ≥ 10 (Druckmann et al., 1982; Otto et al., 1989; Braiman et al., 1991; Pfefferlé et al., 1991; Maeda et al., 1992), i.e., unusually high. Indirect evidence suggests that the pK_a of the Schiff base is lowered considerably as it becomes the proton donor in the L to M reaction to the low-pK_a residue D85. In halorhodopsin, a related retinal protein, measurements of the rates of base-catalyzed Schiff base deprotonation and reprotonation during the photocycle indicated that the Schiff base pK_a was lowered transiently from about 7.5 to 4.3 (Lanyi, 1986). If a similar but larger change occurs in bacteriorhodopsin while the pK_a of D96 remains unchanged, the pK_a of the Schiff base would have to rise strongly during the M state so as to allow the ensuing proton transfer from D96. Alternatively, the pK_a of D96 is lowered, or a combination of both of these pK_a changes occurs. However, the possibility of any changes in the proton affinity of D96 during the photocycle has been so far unexplored.

When deprotonation of the Schiff base is prevented, either because (1) D85 cannot function as proton acceptor, e.g., at low pH where the residue is already protonated (Mowery et al., 1979; Fischer & Oesterhelt, 1979; Váró & Lanyi, 1989; Subramaniam et al., 1990) or when D85 is replaced by a nonprotonable group (Subramaniam et al., 1990), or (2) the pK_a's of D85 and the Schiff base are altered relative to one another, e.g., in the D212N protein at pH >6 (Needleman et al., 1991), the photocycle does not contain an M state. In such cases, and particularly in case 2, the photocycle is described by the generic scheme $BR \xrightarrow{h\nu} K \leftrightarrow L \leftrightarrow N \rightarrow BR$. According to FTIR spectra (Braiman et al., 1992), what was first termed as a kinetically distinct second L state in D212N (Needleman et al., 1991) is an N state very similar to N in the wild-type photocycle. The following question arises therefore: Does D96 deprotonate in the N intermediate under these conditions, i.e., without prior deprotonation of the Schiff base? The FTIR spectra indicate that it does, and in this report we confirm that the proton originates from D96 and show that after a delay it is released to the bulk. The driving force for the deprotonation of D96 in the wild-type therefore cannot be solely the proton affinity of the deprotonated Schiff base; there occurs a transient lowering of the pK_a of D96 independent of the Schiff base.

A similar question can be asked about the dependence of a protein backbone conformation change, detected as changes in the amide I and II bands in the wild-type photocycle, on the protonation state of the Schiff base. These difference bands have been demonstrated in N (Braiman et al., 1987, 1991; Ormos, 1991; Ormos et al., 1992; Pfefferlé et al., 1991), but when the M to N reaction is slow, as in the D96N protein at high pH, they appear already in an M substate termed M_N (Sasaki et al., 1992). We find that the amide bands appear in the D212N photocycle also, i.e., without prior Schiff base deprotonation. The protein change they reveal is concurrent with the deprotonation of D96 in N as in wild-type. Consistent with a recent suggestion based on different arguments (Sasaki et al., 1992), we suspect that the deprotonation is tightly coupled to the backbone conformation change. The thermodynamics of the chromophore reactions during the conformational change indicate that the amide bands are not directly related to the switch reaction of the pump.

MATERIALS AND METHODS

Halobacterium halobium containing the recombinant D212N/D96N gene for bacteriorhodopsin was constructed using a shuttle vector described before (Ni et al., 1990; Needleman et al., 1991). Both D212N (Needleman et al., 1991) and D212N/D96N bacteriorhodopsins were prepared as purple membrane sheets, by a standard method (Oesterhelt & Stoeckenius, 1974). Unless otherwise mentioned, all experiments were done at room temperature.

Time-resolved spectroscopy in the visible and analysis of the difference spectra to derive component spectra and kinetics were described before (Zimányi et al., 1989; Váró & Lanyi, 1991a,c). Single-wavelength measurements were as described elsewhere (Váró & Lanyi, 1990b), except that the samples were encased in polyacrylamide gels (Mowery et al., 1979). In the determinations of transient pH changes with pyranine, the time-dependent absorption change at 457 nm was recorded in unbuffered gels, followed by addition of $^1/_{25}$th volume of 0.5 M phosphate to the gel bathing solution, adjusted to a pH which would give the same pH upon dilution to 20 mM as the initial solution, and incubation in the dark for 1 h to equilibrate the buffer with the gels. Subtraction of the second trace from the first gave the absorption changes due to the dye. To avoid effects due to anion binding near the Schiff base, such as described by Marti et al. (1991), the experiments were carried out in the presence of Na_2SO_4 rather than NaCl. Only in the study of the temperature dependencies of the rate constants was NaCl used, for the reason that we wished to compare the results with earlier data on the wild-type photocycle (Váró & Lanyi, 1991a).

Time-resolved FTIR difference spectroscopy was performed using a stroboscopic technique as described previously (Braiman et al., 1991). Briefly, each purple membrane sample was washed 3 times in 50 mM NaCl/10 mM Tris·HCl, pH 8.0, and then pelleted at 5000*g*. The pellet was partially dried under a steam of dry air and sealed between CaF_2 windows. The final water content was estimated on the basis of the IR spectra to be ca. 50% by weight. Two different types of measurements were made, covering different time ranges after the 530-nm flash-excitation. First, the range 20 μs–2 ms was covered with 20-μs spacing between digitizations of the interferogram, collecting 99 interferogram points after each flash and sorting these points one at a time into different files. Second, the range 180 μs–30 ms was covered with 15-μs spacing between digitizations, collecting 2000 interferograms after each flash and sorting these points 8 at a time into different files. For both time ranges, the spectral resolution was 4 cm^{-1} and the bandwidth was 0–1900 cm^{-1}.

The singular value decomposition method (SVD; Golub & Kahan, 1992), used for analyzing the IR difference spectra, was utilized also for noise-filtering the visible and the infrared spectra. For this calculation, the time-resolved spectra were converted to a set of SVD spectra, each with accompanying kinetics. Since only a few of these contained real features, the original spectra could be regenerated from these alone, leaving out all the other SVD spectra and the noise they contributed to the data.

Cell envelope vesicles containing D212N bacteriorhodopsin were prepared by sonication of *H. halobium* cells and light-driven proton transport assayed as before (Needleman et al., 1991), except that a saturating light intensity was used. The ionic conditions were adjusted to obtain transport activity at pH 5.0 with 1.4 M Na_2SO_4 *plus* 160 mM NaCl (purple chromophore) as a control, and transport was then tested at pH 7.2 with 1.5 M Na_2SO_4 (blue chromophore). The vesicle protein concentration in the assays was 0.8 mg/mL.

RESULTS

Photocycles of the Blue Forms of D212N and D212N/D96N Bacteriorhodopsins. The D212N residue replacement has the consequence that at pH >6 the absorption maximum of the chromophore is shifted from 568 nm to about 585 nm; in contrast with the purple form at pH <6, the photocycle of this blue form does not contain an M intermediate (Needleman et al., 1991). We repeated the earlier measurements of this photocycle, but the quality of the time-resolved difference spectra is now much improved by removing random noise with SVD filtering. Figure 1 shows such filtered spectra for D212N bacteriorhodopsin. The grouping of the spectra into three time domains (panels A–C) makes it evident that three distinct isosbestic points, at 573, 560, and 547 nm, appear during the chromophore reaction sequence. The third isosbestic point lies on the zero line, indicating that it reflects recovery of the initial BR state. The spectra were nearly stationary between the first and the second, and the second and the third time domains shown. Thus, there are three spectroscopically distinct transformations in this photocycle which do not overlap greatly in time. They correspond to the K ↔ L, L ↔ N, and N → BR reactions (cf. below).

In Figure 2, time-resolved difference spectra are given for D212N/D96N bacteriorhodopsin. The data are strikingly similar to those for D212N (compare with the spectra in Figure 1), except for two kinetic features. The quasi-stationary state between K and L, which develops for D212N/D96N at about 10 μs, contains more K (absorption in the red) than that for D212N, and the decay of the final intermediate (i.e., N, cf. below) to BR is 6–7 times slower.

Using the method described earlier (Váró & Lanyi, 1991a,b,c) and taking the isosbestic points in Figure 1 into account, spectra were found for the intermediates for the D212N photocycle, which both satisfied simple criteria for the shape of rhodopsin spectra in general and gave kinetics which could be fitted with a simple model in which the sums of the intermediates present did not significantly deviate from 1 until the initial BR state began to repopulate. The spectra for the intermediates K, L, and N in the D212N system, and their time-dependent concentrations, are shown in Figure 3. The maximum for BR is at 580 nm (Needleman et al., 1991), and for K, L, and N at 603, 560, and 550 nm, respectively (Figure 3A). The maximum for K is red-shifted, and for L and N blue-shifted from BR, as in the wild-type. The maxima of what we now call L and N were earlier described as coincident (Needleman et al., 1991), but with improved signal/noise, they are seen to be somewhat shifted relative to one another. Unexpectedly, the direction of this shift is the reverse of that in wild-type. The kinetics (points in Figure 3B) are consistent with the model K ↔ L ↔ N → BR (lines). The rate constants (legend for Figure 3) indicate that neither the K ↔ L nor the L ↔ N reaction occurs very far from equilibrium.

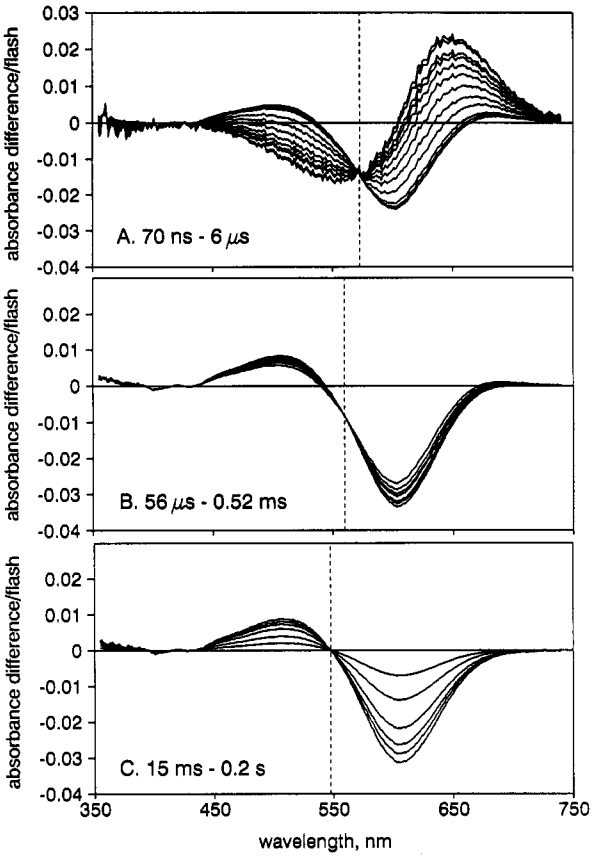

FIGURE 1: Difference spectra measured after photoexcitation of D212N bacteriorhodopsin at increasing delay times. Conditions: 20 μM bacteriorhodopsin, 1 M Na_2SO_4, 20 mM phosphate, pH 6.9, 22 °C. Delay times: (A) (in order of decreasing positive amplitude at 650 nm), 70 ns, 100 ns, 210 ns, 310 ns, 450 ns, 650 ns, 940 ns, 1.4 μs, 2 μs, 2.9 μs, 4.2 μs, and 6 μs; (B) (in order of increasing negative amplitude at 600 nm), 56, 81, 120, 170, 250, 360, and 520 μs; (C) (in order of decreasing amplitude), 15, 21, 31, 45, 94, and 200 ms. The raw difference spectra were very similar to those published earlier (Needleman et al., 1991); the spectra are shown after removing a large part of the noise by converting the data to a set of SVD spectra (Golub & Kahan, 1992) and reconstructing them from only those which contained nonrandom spectral features. In the time domains between 6 and 56 μs, and 520 μs and 15 ms, the spectra very virtually stationary, and are not shown. Isosbestic points are indicated with dashed lines.

Proton Release and Uptake in the Blue Forms of D212N and D212N/D96N Bacteriorhodopsins. Near neutral pH, the net translocation of protons in the photocycle of wild-type bacteriorhodopsin is accomplished by release of a proton on the extracellular side, followed by uptake on the cytoplasmic side (Lozier et al., 1976). The transient appearance of protons in the bulk can be detected by following the absorption change with time due to protonation of dyes such as pyranine, a negatively charged pH indicator (Grzesiek & Dencher, 1986, 1988; Heberle & Dencher, 1990, 1992; Otto et al., 1989, 1990). We measured the absorption change at 457 nm in the presence of pyranine at pH 6.9, first without added buffer and then with 20 mM phosphate set to the same pH; the change of pyranine absorption was obtained by subtracting the second trace from the first. Figures 4 and 5 show time-dependent

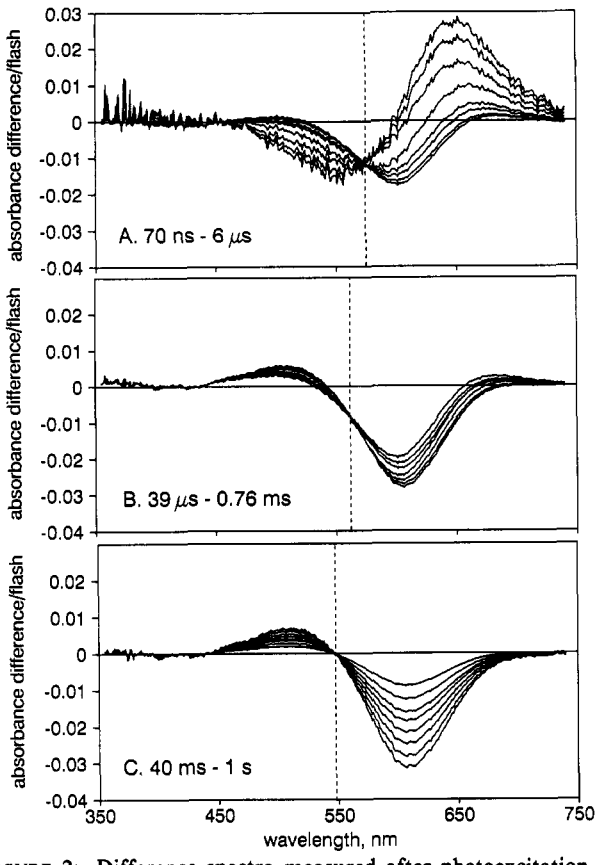

FIGURE 2: Difference spectra measured after photoexcitation of D212N/D96N bacteriorhodopsin at increasing delay times. Conditions as in Figure 1. Delay times: (A) (in order of decreasing positive amplitude at 650 nm), 70 ns, 100 ns, 210 ns, 450 ns, 940 ns, 1.4 μs, 2.9 μs, and 6 μs; (B) (in order of increasing negative amplitude at 600 nm), 39, 56, 81, 120, 170, 360, and 760 μs; (C) (in order of decreasing amplitude), 40 ms, 60 ms, 100 ms, 150 ms, 250 ms, 400 ms, 600 ms, and 1 s. The spectra are shown after removing a large part of the noise by converting the data to a set of SVD spectra as in Figure 1, and reconstructing them from only those which contained nonrandom spectral features. As discussed in the text, the kinetics in this photocycle are very similar to those in D212N (Figure 1). Isosbestic points are indicated with dashed lines.

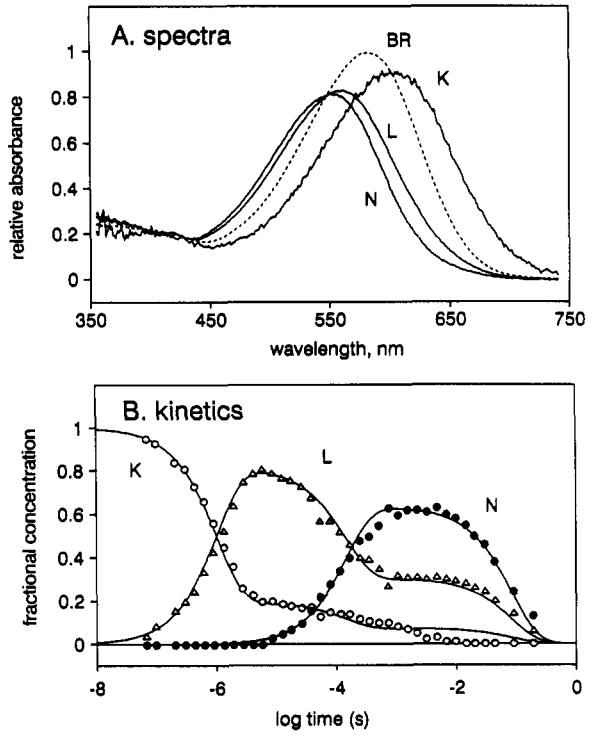

FIGURE 3: Reconstructed spectra and kinetics for the D212N photocycle. The data used are given in part in Figure 1. (A) Calculated spectra for BR (initial state, dashed line) as well as the photointermediates K, L, and N. (B) Calculated concentrations of K (○), L (△), and N (●) as functions of delay time after photoexcitation, and best fit of the scheme K ↔ L ↔ N → BR (lines). Rate constants (in s^{-1}): $k_{KL} = 7.7 \times 10^5$; $k_{LK} = 1.8 \times 10^5$; $k_{LN} = 5.3 \times 10^3$; $k_{NL} = 2.5 \times 10^3$; $k_{NBR} = 18$.

absorption changes at 410 nm (kinetics for the deprotonated Schiff base, i.e., M), at 570 nm (a weighted sum of the kinetics for all species with a protonated Schiff base, i.e., K, L, and N), and the net dye kinetics at 457 nm. In wild-type bacteriorhodopsin (Figure 4), the kinetics of the proton are described approximately by the time constants of 260 μs and 15 ms for release and uptake, respectively. As found earlier, the proton release measured in this way lags behind the rise of M (here with an overall time constant of about 100 μs) because pyranine detects protons in the bulk rather than at the surface (Heberle & Dencher, 1992). The proton uptake correlates with the decay of N (Kouyama et al., 1988; Váró & Lanyi, 1990b); under the conditions in Figure 4, this contributes only a minor part of the rise in absorbance at 570 nm which is dominated by a larger change due to the decay of M. Although stoichiometry was not determined here, in other experiments of this kind about 1 proton per M had been detected (Grzesiek & Dencher, 1986; Drachev et al., 1984; Váró & Lanyi, 1990b).

With D212N bacteriorhodopsin, the results are different (Figure 5A). As predicted from the spectra of the intermediates in Figure 3A, which are seen to overlap the spectrum of bacteriorhodopsin considerably, the absorption decrease at 570 nm is about half the amplitude of that in wild-type. The absence of an absorption change at 410 nm indicates that with approximately the same amount of chromophore photoexcited as wild-type no detectable M is produced (compare Figures 4 and 5A). A proton is released, however, but at a later time in the photocycle than in the wild-type system. The proton release occurs under these conditions with a time constant of 2 ms; it is delayed relative to the nearest chromophore reaction, the accumulation of the N intermediate, which has a time constant of 220 μs (Figure 3B). This delay is too long to originate from transfer of the released proton from the surface to the bulk. It indicates that an additional transition not detectable in the visible (but detectable in the infrared, cf. below) takes place. These measurements resolve, therefore, an N′ state which follows N with a time constant of about 2 ms. The subsequent uptake of the proton is with a time constant of 160 ms. This is comparable to the time constant of the N → BR reaction which is 130 ms from the absorption change at 570 nm in Figure 5A. The amount of protons released per N′ is about the same as protons per M in wild-type (i.e., about 1), indicating that the proton detected originates from a group which nearly completely deprotonates in N′. Since the pH of these measurements is 6.9, we conclude that the pK_a of this group (D96, cf. below) is below 7 at the time of proton release.

Although the D212N photocycle is changed by introduction of the additional residue replacement D96N only in that the K ↔ L equilibrium contains more K and the recovery of BR is slower, as Figure 5B shows there is no proton exchange with the bulk in this system. The simplest explanation, supported by the FTIR spectra (cf. below), is therefore that the released proton originates from D96. Likewise, no protons were detected with pyranine after photoexcitation of D85N bacteriorhodopsin (not shown), even though its photocycle

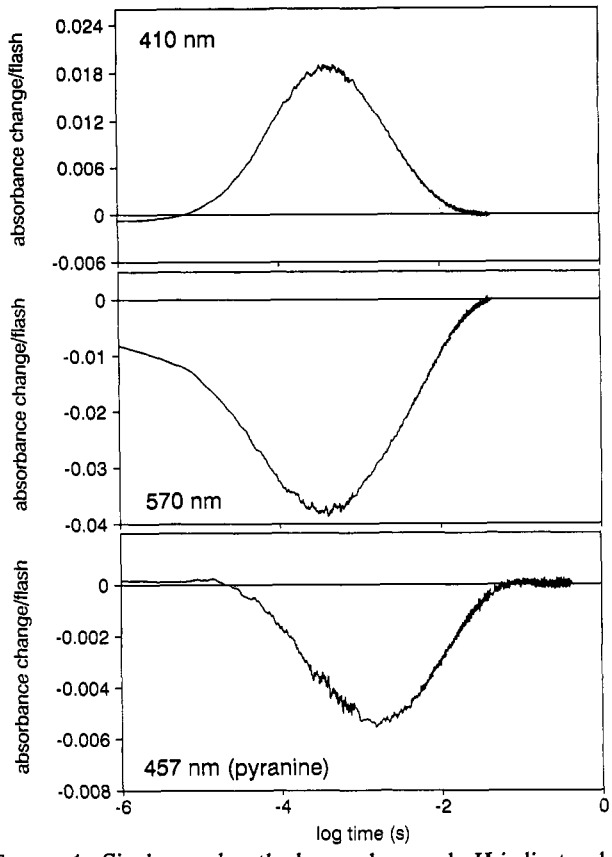

FIGURE 4: Single-wavelength chromophore and pH indicator dye kinetics for wild-type bacteriorhodopsin. Conditions as in Figure 1, but the absorbance at the indicated wavelength was recorded as a function of delay time after photoexcitation. In the dye experiments, 100 μM pyranine was present, and the trace shown is the difference between a recording without buffer and another with added phosphate (to 20 mM, adjusted to give pH 6.9 upon dilution).

resembles that of the red-shifted form of D212N.[1] The reason for this result is less clear, however.

Transport Activity of the Blue Form of D212N Bacteriorhodopsin. Light-driven proton transport was measured in cell envelope vesicles under conditions where either the blue or the purple form of D212N predominates (cf. Materials and Methods). The initial rate of proton extrusion from vesicles at pH 5.0, containing the purple form, was 15.8 ± 3.2 nmol of H^+ min^{-1} (mg of protein)$^{-1}$; transport activity under similar conditions was about 30% that of wild-type, compared on the basis of bacteriorhodopsin content (Needleman et al., 1991). The same vesicles at pH 7.2, containing the blue form, in contrast exhibited a measurable but very small proton extrusion rate at 0.15 ± 0.02 nmol of H^+ min^{-1} (mg of protein)$^{-1}$, i.e., about 1% of the vesicles with the purple form. This will have originated from a small amount of purple chromophore in the mixture. Photovoltage kinetics measured with the blue form of the D212N protein indicate likewise no net charge translocation in the photocycle (Moltke et al., 1993). We conclude, therefore, that the BR $\xrightarrow{h\nu}$ K ↔ L ↔ N (→N′) → BR photocycle of D212N does not transport protons. This is as expected, because in wild-type bacteriorhodopsin the deprotonation of the Schiff base is a requirement for proton transport (Longstaff & Rando, 1987).

Thermodynamics of the D212N Photocycle. For the wild-type photocycle, the enthalpy and entropy levels of the intermediates could be reconstructed (Váró & Lanyi, 1991a) from the temperature dependencies of the elementary rate constants and calorimetric data in the literature (Ort & Parson, 1979; Garty et al., 1982; Birge & Cooper, 1983; Birge et al., 1991). The $M_1 \rightarrow M_2$ transition is distinguished by large changes in free energy, enthalpy, and entropy. Before this reaction, excess free energy is mostly in the form of enthalpy, while afterward it is in the form of negative entropy. The originally suggested physical meaning of this enthalpy/entropy conversion was that in M_2 the Schiff base pK_a will have returned to its high initial value, but at the expense of a restricted protein conformation whose relaxation drives the completion of the cycle (Váró & Lanyi, 1991a). The appearance of amide bands in FTIR difference spectra appeared to support this interpretation, because it indicated that a conformational change does, in fact, take place. The details of the $M_1 \rightarrow M_2$ reaction have been recently refined, however: (1) part of the free energy dissipation step is now attributed to the release of the transported proton on the extracellular side, which makes the reaction unidirectional when the pH is well above the pK_a of the proton release group (Zimányi et al., 1992b); (2) the FTIR amide bands are now suggested to reflect a protein backbone change which occurs after the switch (Sasaki et al., 1992).

The rate constants of the D212N photocycle lacking M were determined at various temperatures under similar conditions as used for the wild-type protein (Váró & Lanyi, 1991a); Figure 6 shows the Eyring plot for the rate constants. The enthalpy of activation for the decay of N is less than all others, as in the wild-type. The calculated enthalpy and entropy cycles are shown in Figure 7. The enthalpy and entropy levels of K and L relative to one another are very similar to those in wild-type [compare with Figure 6 in Váró and Lanyi (1991a)]. However, in other respects the thermodynamic parameters are dramatically different in the two systems. As Figure 7 shows, in D212N the enthalpy and entropy contents were *increased* in N relative to L, by about 10 kJ/mol and 50 J/(mol·K), respectively, rather than *decreased* by about 60 kJ/mol and 150 J/(mol·K), respectively, as in wild-type. Thus, in D212N the excess free energy acquired in K remains predominantly as enthalpy throughout. The thermodynamics in the absence of Schiff base deprotonation do not reveal, therefore, the occurrence of an energetically relevant large protein conformational change. Since the amide bands are still observed under these conditions (cf. below), their interpretation will have to take this into account.

In D212N, and particularly D212N/D96N, the N → BR reaction is considerably slowed relative to wild-type. Interestingly, Figure 7B indicates that the primary barrier to this reaction is entropic. The entropy of the transition state is low and nearly the same as in wild-type, in spite of the much more positive entropy of N [compare with Figure 6 in Váró and Lanyi (1991a)]. Thus, the recovery of BR, limited in this case probably by the reisomerization of the retinal, takes a similar path in the two systems, one which is characterized by a restricted protein conformation. This, and the suggested structural role for D96 (Thorgeirsson et al., 1991), might explain the unexpected slow N → BR reaction in the two mutated proteins.

Time-Resolved FTIR Difference Spectra in the Photocycles of D212N and D212N/D96N Bacteriorhodopsins. The L → N, N → N′, and N′ → BR processes observed in the visible or by means of the pH-indicator dye were seen also in the infrared. The time courses obtained from the SVD analysis of time-resolved FTIR spectra of the D212N sample are shown in Figure 8. The data in Figure 8A,B, covering the time range under 2 ms, show clearly the L → N transition; the best-fit

[1] Váró, Cao, and Lanyi, unpublished experiments.

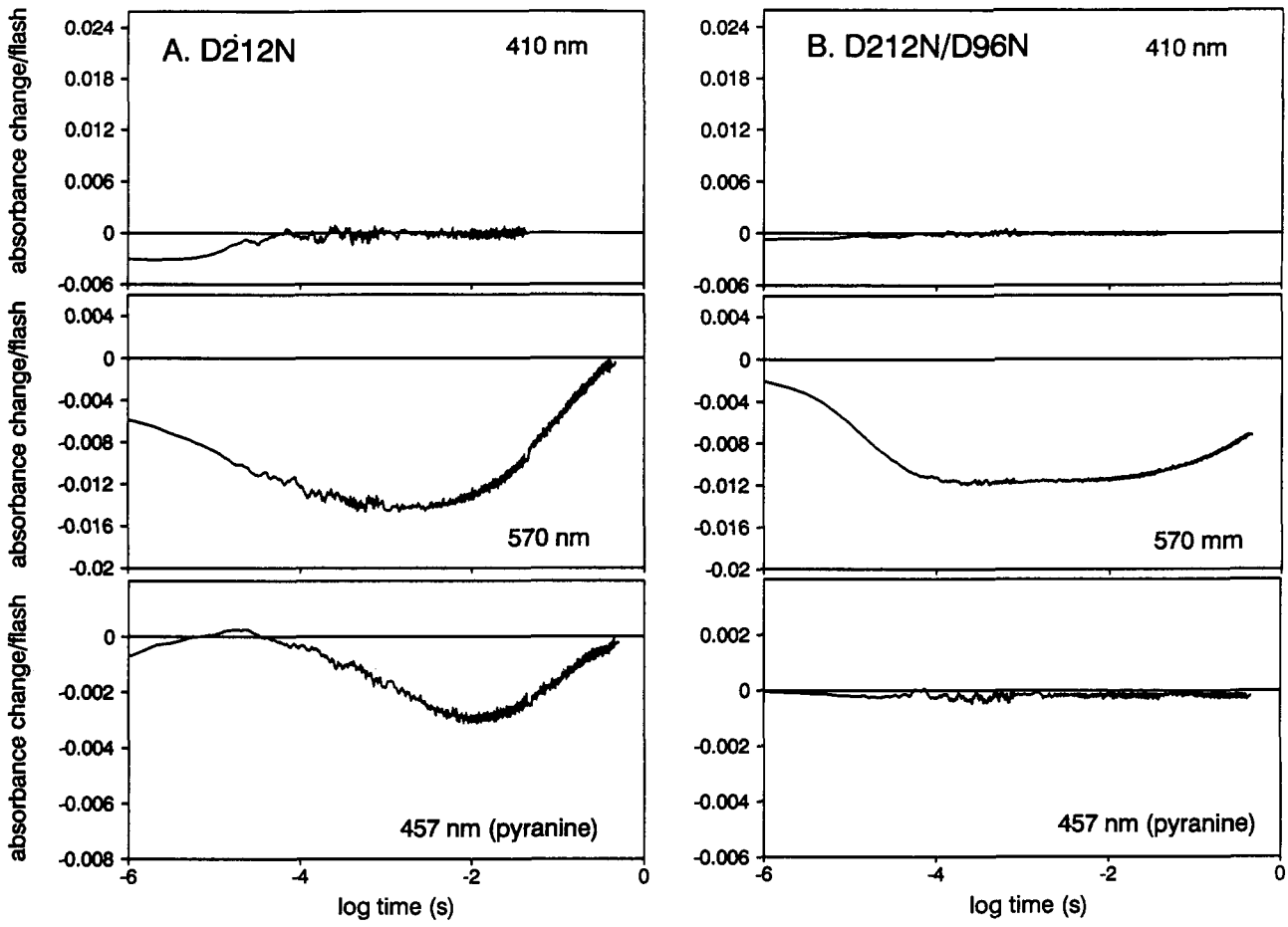

FIGURE 5: Single-wavelength chromophore and pH indicator dye kinetics for D212N (A) and D212N/D96N (B) bacteriorhodopsins. Conditions as in Figure 4.

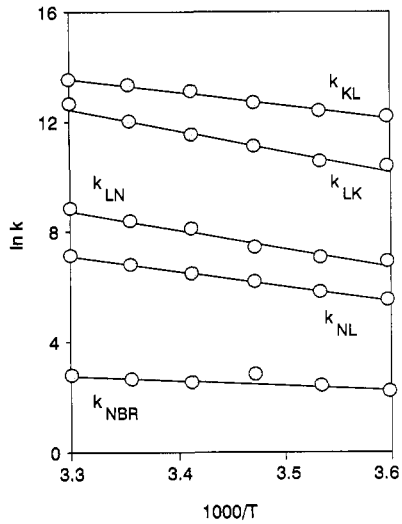

FIGURE 6: Eyring plot for the rate constants of the photocycle of the blue form of D212N. Conditions: 25 μM bacteriorhodopsin, 100 mM NaCl, and 50 mM phosphate, pH 8.0, at 5, 10, 15, 20, 25, and 30 °C. The time-dependent concentrations of K, L, and N after photoexcitation at each of the six temperatures were calculated with component spectra derived from the measured difference spectra at 20 °C. Because the spectra of L and N are very similar (Figure 3A), in this analysis the sum of [L] and [N] as a function of time was calculated rather than [L] and [N] individually as in Figure 3B. The rate constants were then obtained by fitting [K] and [L + N] to the model in the text. The equivalent Eyring plot for wild-type is given in Figure 5 of Váró and Lanyi (1991a).

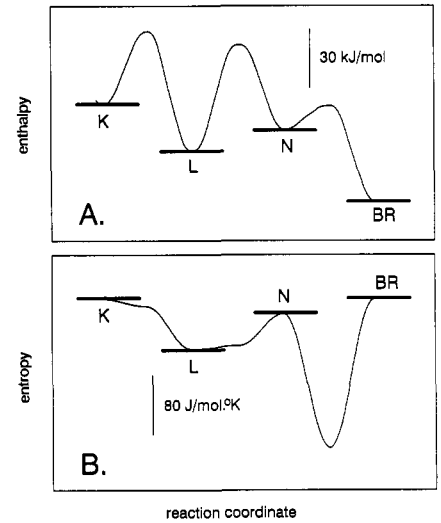

FIGURE 7: Enthalpy (A) and entropy (B) cycles of the blue form of D212N. Calculations from the data in Figure 6, as in Váró and Lanyi (1991a). The assumptions were that the excess enthalpy of K is the same as in wild-type, i.e., about 50 kJ/mol (known from a calorimetric determination (Birge et al., 1991), and that entropy changes in K are negligible compared to those which occur later in the photocycle (Váró & Lanyi, 1991a). The equivalent plots for wild-type are given in Figure 6 of Váró and Lanyi (1991a).

time constant for this process was 146 ± 10 μs, which corresponds to the 220-μs time constant in the visible, given the somewhat different sample conditions required for the infrared measurement. The K → L transition was not resolved. Fitting the decay of L to exponentials required at least one more time constant which was under 3 ms, but the time range covered was too short to give a value more precisely. From these data, it was possible to deconvolute approximately the contributions of L and N to the difference spectra in the <2-

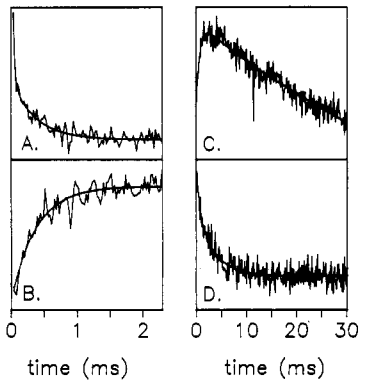

FIGURE 8: Time courses for the amplitudes of the two most significant spectral components obtained by SVD for the D212N photoreaction. Each dimensionless SVD time course represents the relative amplitude of the associated basis spectrum at each time, determined as the overlap of the calculated basis spectrum with the measured spectrum at that time. The SVD time courses give the same decay time constants as would individual spectral peaks, but they are "averaged" (in a certain sense) over the entire spectral frequency range in order to improve the signal/noise ratio. Two different time ranges were examined: (A and B) 20 μs–2 ms, with a temporal spacing of 20 μs between spectra; (C and D) 180 μs–30 ms, with a temporal spacing of 122 μs. Each pair of time courses was fit to a multiexponential decay. The fitted time constants were as follows: (A and B) 146 ± 50 μs and a second time constant <3 ms; (C and D) 700 ± 200 μs (corresponding to an instrumental time constant), 3.7 ± 0.9 ms, and 122 ± 14 ms.

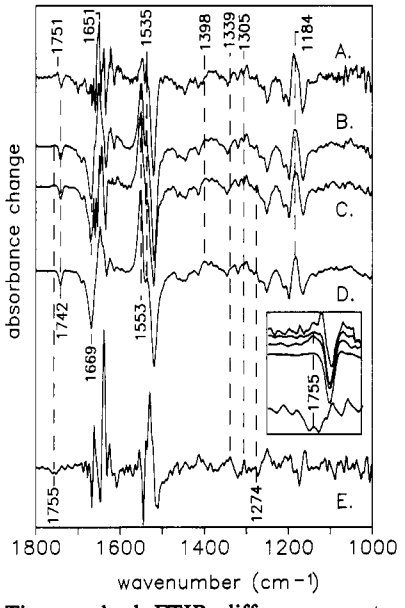

FIGURE 9: Time-resolved FTIR difference spectra of D212N corresponding to (A) the BR → L, (B and C) BR → N, (D) BR → N′, and (E) N → N′ reactions. Spectrum E is the difference between (C) and (D). Spectra A and B were derived from data obtained between 20 μs and 2 ms; spectra C and D were from data between 2 and 30 ms. Inset: an expanded version of the same spectra showing the region from 1800 to 1700 cm^{-1}. The spectra are plotted in the same vertical order as in the main figure.

ms time range, using procedures described previously (Chen & Braiman, 1991). The resulting BR → L and BR → N difference spectra are given in Figure 9A and Figure 9B, respectively.

The data in Figure 8C,D cover the time range of 180 μs–30 ms, and allow clear detection of the N → N′ reaction which was inferred from the dye kinetics. This spectral decay process with a time constant of 3.7 ± 0.5 ms can be discerned most clearly in the second component of the SVD analysis of the long time range (Figure 8D). The time constant corresponds approximately to the 2-ms time constant for proton release

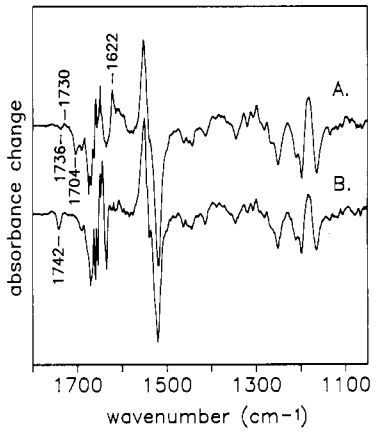

FIGURE 10: Time-resolved FTIR difference spectra of the BR → N photoreaction of (A) D212N/D96N and (B) D212N. Spectrum B is identical to Figure 9C; spectrum A was obtained in the same way from the double-mutated protein, which also showed an L → N transition with a time constant of 136 μs.

into the bulk medium (Figure 5A). In addition, there was a spectral decay with a time constant of 122 ± 14 ms, seen most clearly in the first component of the SVD analysis of the long time range (Figure 8C). It must correspond to the recovery of the initial bacteriorhodopsin state observed in the visible.

It is clear that the BR → N difference spectra calculated from data covering two different time ranges (Figure 9B,C) are quite similar, indicating that the assumptions which underlie their calculation are reasonably accurate. These spectra are also very similar to previously published BR → N difference spectra for wild-type bacteriorhodopsin (Braiman et al., 1991; Bousché et al., 1991; Pfefferlé et al., 1991), showing the positive peaks at 1184, 1398, 1535, 1553, and 1651 cm^{-1} and the negative peaks at 1669 and 1742 cm^{-1} characteristic of this intermediate. The spectrum for N differs in two important respects from the spectrum of L: in the amide bands which indicate a protein backbone conformational change in N, and in the COOH bands which correspond to changes in aspartate residues. The amide I bands at 1651 and 1669 cm^{-1}, and the amide II band at 1553 cm^{-1}, are clearly evident in N (Figure 9B). The presence of the 1742-cm^{-1} negative peak, assigned on the basis of site-directed mutagenesis to deprotonation of the COOH group of D96 in N (Gerwert et al., 1989; Bousché et al., 1991), indicates that D96 deprotonates in the N intermediate of D212N despite the absence of its usual proton acceptor, i.e., the unprotonated Schiff base of the M intermediate. We confirmed the assignment of this peak to D96 in the D212N protein by obtaining a BR → N difference spectrum also after D212N/D96N double-residue replacement (Figure 10A). The additional mutation causes disappearance of the 1742-cm^{-1} negative COOH band without changing significantly most of the rest of the spectrum. The new 1704-cm^{-1} negative band is attributable to perturbation of the carbonyl group of N96, on the basis of its previous observation in the D96N single mutant (Maeda et al., 1992). For the same reason, the new 1622-cm^{-1} positive band is probably due also to an N96 vibration which had not been assigned specifically. The spectrum of the L intermediate of D212N contains the 1742-cm^{-1} negative band as well, but the appearance of a distinct positive peak at 1751 cm^{-1} (Figure 9A, and inset) suggests that its cause is a shift rather than the disappearance of the COOH vibration. Thus, the FTIR difference spectra demonstrate that in D212N the residue D96 is protonated, probably to a large extent, in L, and that it deprotonates during the L → N reaction.

Deprotonation of D96 between the L and N states is expected to result in positive FTIR difference bands due to symmetric and antisymmetric COO^- vibrations in the 1300–1400- and ~1560-cm^{-1} regions, respectively. A positive band, observed near 1398 cm^{-1} in the BR → M spectrum of D212N (Figure 9B,C), has been previously attributed to the D96 COO^- symmetric stretch vibration in the wild-type (Braiman et al., 1990; Bousché et al., 1991; Maeda et al., 1992). However, this assignment is not definitive, and is somewhat contradicted by the relatively small changes observed in this frequency region when D96 is replaced (see Figure 10A,B). There are other bands in the 1300–1400-cm^{-1} region of the BR → N and BR → N′ difference spectra (Figure 9B–D) that could be assigned to this D96 COO^- vibration. Despite the absence of a definitive assignment for this vibration, deprotonation of D96 during the L → N transition provides the best explanation for the observed spectral changes in the 1740–1760-cm^{-1} region.

The dye experiments indicate that this proton is not released into the medium until the formation of N′. Thus, between 150 μs and 2 ms, the proton is latent, being no longer on D96 but not yet in the bulk. We examined the FTIR spectra of the N and N′ intermediates for evidence of another proton acceptor. The most likely candidate seemed to be D85 which is normally protonated in the N state (Braiman et al., 1991; Bousché et al., 1991) and therefore can be expected to have a sufficiently high pK_a to serve as proton acceptor to D96. However, in D212N the positive N → BR difference band at 1755 cm^{-1} (which in wild-type is attributable to the COOH group of D85) is much reduced in intensity. This indicates that a pH 8, at least, in this protein D85 is mostly unprotonated in the N state, a fact easily rationalized since under these conditions no M is formed, and it is in the M state where D85 accepts a proton from the Schiff base (Braiman et al., 1988a). Evidently, eliminating the M state in D212N largely eliminates protonation of D85.

Nevertheless, a small band is observed at 1755 cm^{-1} in the BR → N difference spectrum (Figure 9, inset), and its presence needs explanation. The clear observation of this peak at 1755 cm^{-1} rather than at 1761 cm^{-1} is a strong indication that it does not arise from a contaminating amount of M intermediate. Thus, D85 must be protonated to a small extent in the N state of D212N via a different mechanism than prevails in the wild-type system. Importantly, the 1755-cm^{-1} band disappears completely during the N → N′ transition (Figure 9, inset). Figure 9E gives a vertically expanded difference spectrum between spectra C and D in Figure 9, corresponding to our best estimate of the N → N′ difference spectrum. It indicates that the proton release has some effects near the chromophore binding pocket, despite the lack of a detectable difference between the spectra of N and N′ in the visible. The negative D85 band at 1755 cm^{-1} is one of the distinct nonchromophoric features in this spectrum, and shows that in the N′ state D85 has lost the small extent of protonation it had acquired in N. There are other (positive) bands in the 1300–1400-cm^{-1} region, e.g., at 1305 and 1339 cm^{-1}, which could be also due to deprotonation of D85. The negative difference band near 1274 cm^{-1} (Figure 9E) is at the frequency assignable to Y185 (Braiman et al., 1988b). However, the small size of this change precludes a significant extent of proton transfer to or from this tyrosine. Clearly, the FTIR spectra do not adequately identify the group which releases the proton during the N → N′ transition, nor the group which accepts the proton from D96 during the L → N transition. It is possible that the proton is transferred from D96 in a delocalized fashion onto several different residues and/or bound water between D96 and D85.

A transient IR continuum absorbance change above 1770 cm^{-1} observed by Gerwert et al. (1990) is also detected in our data. The average values of the spectral base line between 1770 and 1800 cm^{-1} ranged from -8.2×10^{-6} (Figure 8B) to -32×10^{-6} (Figure 8C); in all cases, these values were in the range of 0.12–0.6% of the size of the negative peak at 1526 cm^{-1}. As pointed out previously (Gerwert et al., 1990), this continuum base-line shift could originate from breaking a network of polarizable hydrogen bonds in the BR state. However, any differences in the size of the negative continuum band between the BR → L, BR → N, and BR → N′ spectra were too small and irreproducible to correlate with any changes in hydrogen bonding near D96 during the L → N reaction.

DISCUSSION

The results in this report indicate that *although the unprotonated Schiff base is normally the proton acceptor for D96, the latter group is destined to deprotonate in the N intermediate even when no unprotonated Schiff base is formed.* In the D212N protein at pH >6, residue D96 deprotonates at the time N is formed and reprotonates as N regenerates the initial BR state. The proton is detected in the bulk with a delay after its loss from D96. The lack of transport under these conditions suggests that this proton is not translocated across the membrane but appears on the cytoplasmic side and is taken up subsequently on the same side. The residue which is the source of the released proton is identified as D96 by the appearance of the 1742-cm^{-1} negative band assigned to D96 in the FTIR difference spectrum of the N intermediate (Figure 9). Lack of this band in the N intermediate of D212N/D96N confirms this interpretation, as does the fact that proton release to the bulk is abolished upon the additional D96N residue replacement (Figure 5B).

The pH dependencies of the reprotonation of the Schiff base (Otto et al., 1989) and the light-dependent loss of a proton from the protein (Renthal, 1981), as well as the persistence of the negative 1742-cm^{-1} band due to changes in an aspartic acid recently established to be D96 in L and N at high pH (Engelhard et al., 1985; Gerwert et al., 1989; Braiman et al., 1991; Pfefferlé et al., 1991; Maeda et al., 1992), indicate that the pK_a of D96 is initially at least 10. This anomalously high pK_a is attributed to the unfavorable free energy of the aspartate anion in the hydrophobic cytoplasmic region of the protein. At the L to M transition, the Schiff base pK_a must be lowered to well below 10 so as to allow proton transfer to D85. In spite of this, the Schiff base is reprotonated from D96 in the N state of the wild-type photocycle, suggesting that the pK_a's of these groups approach one another again. The results we report here demonstrate that residue D96 deprotonates at about this time after photoexcitation even when the Schiff base is protonated. Thus, the reason for the proton exchange between D96 and the Schiff base in N cannot be solely the increased proton affinity of the Schiff base but must reside at least partly in a transient decrease of the pK_a of D96 to below 7. The cause of the decrease of this pK_a must be in a change of the dielectric environment of D96.

In general, the pK_a of a buried aspartate is lowered when the anionic carboxylate is stabilized, either through increased interaction with a positive protein residue or through increased hydration. The first alternative invokes transiently increased charge interaction between D96 and R227. Indeed, replacement of R227 with glutamine slows Schiff base reprotonation

considerably (Stern & Khorana, 1989). This would be consistent with an M ↔ N equilibrium which is shifted toward M, although other explanations are also possible. There is some evidence for the second alternative as well, i.e., that hydration near D96 plays a role in reprotonating the Schiff base. Earlier results indicated that dehydration by osmotically active solutes (Cao et al., 1991) and lowered humidity (Váró & Lanyi, 1991b) inhibited specifically the rate of the M to N reaction, an effect explained by the necessity for internally bound water for stabilizing the transition state in the D96 to Schiff base proton transfer. Although a net increase of bound water in the protein during the formation of N is unlikely in view of the insensitivity of the $M_2 \leftrightarrow N$ equilibrium constant to osmotic agents in the wild-type system (Cao et al., 1991), and the lack of entropy decrease associated with the $L \rightarrow N$ reaction in D212N (Figure 7B), a changed arrangement of internal hydration might be necessary for stabilizing the D96 aspartate anion. Thus, either rearrangement of bound water in the cytoplasmic region of the protein or closer contact of D96 and R227, caused by minor tilting or kinking of one or more of the transmembrane helices (Glaeser et al., 1986; Dencher et al., 1989), would be plausible mechanisms for lowering the pK_a of D96 in the N state. We suggest that for one or both of these reasons, and regardless of the state of the Schiff base, the proton of D96 will dissociate in the N intermediate, and find itself in the cytoplasmic proton channel. In the wild-type, this proton is captured by the deprotonated Schiff base, but in D212N it is retained in the protein, partly by D85 and partly by other unidentified groups, and released to the bulk after a delay of somewhat less than 2 ms through nonspecific leak pathways.

The amide I and II bands characteristic of the M_N (Sasaki et al., 1992) and N (Braiman et al., 1987, 1991; Ormos, 1991; Ormos et al., 1992; Pfefferlé et al., 1991) states in M-containing photocycles appear in the N state of the D212N photocycle also (Figure 9). The backbone conformational change which gives rise to these bands is clearly not dependent on deprotonation of the Schiff base. It appears, therefore, that its cause is not the chromophore reaction which normally precedes it but the strains introduced into the protein by the initial isomerization of the retinal much earlier in the photocycle. The protein will have responded with a delay to the changed geometry of the retinal, unrelated to intervening events involving the chromophore. Coincidence of retinal and protein changes in the infrared had suggested tight coupling of chromophore and protein (Gerwert et al., 1990). The results with the D212N protein suggest, however, that it is justified to refer to a "protein conformation cycle" and a "D96 deprotonation cycle", which are parallel to but to some degree independent of the "chromophore cycle". Recently we made a similar suggestion about the lack of strict coupling between deprotonation reactions near the extracellular protein surface and the chromophore cycle (Zimányi et al., 1992b).

On the other hand, a direct connection between the changed pK_a of D96 in the N intermediate and the amide bands in the FTIR spectra seems very likely. Because in D96N at pH 10 the amide I and II bands appeared together with perturbation of N96 and already in the M_N state, a novel intermediate placed tentatively between M_2 and N, Sasaki et al. (1992) suggested that in the wild-type photocycle the role of the protein backbone change might be to allow proton transfer from D96 to the Schiff base. The results in this report are in agreement with this interpretation. Although the protein conformation change detected by FTIR has been proposed as the candidate for the switch reaction of the pump (Fodor et al., 1988; Ormos, 1991), the thermodynamics of the D212N system (Figure 7) indicate that the amide bands are observable in N without the characteristic entropy decrease associated with the switch. It appears, therefore, that the entropy decrease (and by implication the switch) does not originate from that protein conformation change which produces the amide bands.

REFERENCES

Ames, J. B., & Mathies, R. A. (1990) *Biochemistry 29*, 7181–7190.

Birge, R. R., & Cooper, T. M. (1983) *Biophys. J. 42*, 61–69.

Birge, R. R., Cooper, T. M., Lawrence, A. F., Masthay, M. B., Zhang, C.-F., & Zidovetzki, R. (1991) *J. Am. Chem. Soc. 113*, 4327–4328.

Bousché, O., Braiman, M. S., He, Y., Marti, T., Khorana, H. G., & Rothschild, K. J. (1991) *J. Biol. Chem. 266*, 11063–11067.

Braiman, M. S., Ahl, P. L., & Rothschild, K. J. (1987) *Proc. Natl. Acad. Sci. U.S.A. 84*, 5221–5225.

Braiman, M. S., Mogi, T., Marti, T., Stern, L. J., Khorana, H. G., & Rothschild, K. J. (1988a) *Biochemistry 27*, 8516–8520.

Braiman, M. S., Mogi, T., Stern, L. J., Hackett, N. R., Chao, B. H., Khorana, H. G., & Rothschild, K. J. (1988b) *Proteins: Struct., Funct., Genet. 3*, 219–229.

Braiman, M. S., Bousché, O., & Rothschild, K. J. (1991) *Proc. Natl. Acad. Sci. U.S.A. 88*, 2388–2392.

Braiman, M. S., Klinger, A. L., & Doebler, R. (1992) *Biophys. J. 62*, 56–58.

Cao, Y., Váró, G., Chang, M., Ni, B., Needleman, R., & Lanyi, J. K. (1991) *Biochemistry 30*, 10972–10979.

Chen, W., & Braiman, M. S. (1991) *Photochem. Photobiol. 54*, 905–910.

Chernavskii, D. S., Chizhov, I. V., Lozier, R. H., Murina, T. M., Prokhorov, A. M., & Zubov, B. V. (1989) *Photochem. Photobiol. 49*, 649–653.

Dencher, N. A., Dresselhaus, D., Zaccai, G., & Büldt, G. (1989) *Proc. Natl. Acad. Sci. U.S.A. 86*, 7876–7879.

Drachev, L. A., Kaulen, A. D., & Skulachev, V. P. (1984) *FEBS Lett. 178*, 331–335.

Druckmann, S., Ottolenghi, M., Pande, A., Pande, J., & Callender, R. H. (1982) *Biochemistry 21*, 4953–4959.

Druckmann, S., Friedman, N., Lanyi, J. K., Needleman, R., Ottolenghi, M., & Sheves, M. (1992) *Photochem. Photobiol. 56*, 1041–1047.

Engelhard, M., Gerwert, K., Hess, B., Kreutz, W., & Siebert, F. (1985) *Biochemistry 24*, 400–407.

Fischer, U., & Oesterhelt, D. (1979) *Biophys. J. 28*, 211–230.

Fodor, S. P., Ames, J. B., Gebhard, R., van der Berg, E. M., Stoeckenius, W., Lugtenburg, J., & Mathies, R. A. (1988) *Biochemistry 27*, 7097–7101.

Garty, H., Caplan, S. R., & Cahen, D. (1982) *Biophys. J. 37*, 405–415.

Gerwert, K., Hess, B., Soppa, J., & Oesterhelt, D. (1989) *Proc. Natl. Acad. Sci. U.S.A. 86*, 4943–4947.

Gerwert, K., Souvignier, G., & Hess, B. (1990) *Proc. Natl. Acad. Sci. U.S.A. 87*, 9774–9778.

Glaeser, R. M., Baldwin, J. M., Ceska, T. A., & Henderson, R. (1986) *Biophys. J. 50*, 913–920.

Golub, G., & Kahan, W. (1992) *SIAM J. Num. Anal. 2*, 205–224.

Grzesiek, S., & Dencher, N. A. (1986) *FEBS Lett. 208*, 337–342.

Grzesiek, S., & Dencher, N. A. (1988) *Proc. Natl. Acad. Sci. U.S.A. 85*, 9509–9513.

Heberle, J., & Dencher, N. A. (1990) *FEBS Lett. 277*, 277–280.

Heberle, J., & Dencher, N. A. (1992) *Proc. Natl. Acad. Sci. U.S.A. 89*, 5996–6000.

Henderson, R., Baldwin, J. M., Ceska, T. A., Zemlin, F., Beckmann, E., & Downing, K. H. (1990) *J. Mol. Biol. 213*, 899–929.

Kouyama, T., Nasuda-Kouyama, A., Ikegami, A., Mathew, M. K., & Stoeckenius, W. (1988) *Biochemistry 27*, 5855–5863.

Lanyi, J. K. (1986) *Biochemistry 25*, 6706–6711.
Lanyi, J. K. (1992) *J. Bioenerg. Biomembr. 24*, 169–179.
Longstaff, C., & Rando, R. R. (1987) *Biochemistry 26*, 6107–6113.
Lozier, R. H., Bogomolni, R. A., & Stoeckenius, W. (1975) *Biophys. J. 15*, 955–963.
Lozier, R. H., Niederberger, W., Bogomolni, R. A., Hwang, S., & Stoeckenius, W. (1976) *Biochim. Biophys. Acta 440*, 545–556.
Lozier, R. H., Xie, A., Hofrichter, J., & Clore, G. M. (1992) *Proc. Natl. Acad. Sci. U.S.A. 89*, 3610–3614.
Maeda, A., Sasaki, J., Shichida, Y., Yoshizawa, T., Chang, M., Ni, B., Needleman, R., & Lanyi, J. K. (1992) *Biochemistry 31*, 4684–4690.
Marti, T., Rösselet, S. J., Otto, H., Heyn, M. P., & Khorana, H. G. (1991) *J. Biol. Chem. 266*, 18674–18683.
Mathies, R. A., Lin, S. W., Ames, J. B., & Pollard, W. T. (1991) *Annu. Rev. Biophys. Biophys. Chem. 20*, 491–518.
Milder, S. J., Thorgeirsson, T. E., Miercke, L. J. W., Stroud, R. M., & Kliger, D. S. (1991) *Biochemistry 30*, 1751–1761.
Miller, A., & Oesterhelt, D. (1990) *Biochim. Biophys. Acta 1020*, 57–64.
Moltke, S., Heyn, M. P., Krebs, M. P., Mollaaghababa, R., & Khorana, H. G. (1993) in *Structures & Functions of Retinal Proteins* (Rigaud, J. L., Ed.) pp 201–204, John Libbey & Company, Paris.
Mowery, P. C., Lozier, R. H., Chae, Q., Tseng, Y. W., Taylor, M., & Stoeckenius, W. (1979) *Biochemistry 18*, 4100–4107.
Nagle, J. F. (1991) *Biophys. J. 59*, 476–487.
Nagle, J. F., & Mille, M. (1981) *J. Chem. Phys. 74*, 1367–1372.
Needleman, R., Chang, M., Ni, B., Váró, G., Fornes, J., White, S. H., & Lanyi, J. K. (1991) *J. Biol. Chem. 266*, 11478–11484.
Ni, B., Chang, M., Duschl, A., Lanyi, J. K., & Needleman, R. (1990) *Gene 90*, 169–172.
Oesterhelt, D., & Stoeckenius, W. (1974) *Methods Enzymol. 31*, 667–678.
Oesterhelt, D., Tittor, J., & Bamberg, E. (1992) *J. Bioenerg. Biomembr. 24*, 181–191.
Ormos, P. (1991) *Proc. Natl. Acad. Sci. U.S.A. 88*, 473–477.
Ormos, P., Chu, K., & Mourant, J. (1992) *Biochemistry 31*, 6933–6937.
Ort, D. R., & Parson, W. W. (1979) *Biophys. J. 25*, 355–364.
Otto, H., Marti, T., Holz, M., Mogi, T., Lindau, M., Khorana, H. G., & Heyn, M. P. (1989) *Proc. Natl. Acad. Sci. U.S.A. 86*, 9228–9232.
Otto, H., Marti, T., Holz, M., Mogi, T., Stern, L. J., Engel, F., Khorana, H. G., & Heyn, M. P. (1990) *Proc. Natl. Acad. Sci. U.S.A. 87*, 1018–1022.
Pfefferlé, J.-M., Maeda, A., Sasaki, J., & Yoshizawa, T. (1991) *Biochemistry 30*, 6548–6556.
Rothschild, K. J. (1992) *J. Bioenerg. Biomembr. 24*, 147–167.
Renthal, R. (1981) *J. Biol. Chem. 256*, 11471–11476.
Sasaki, J., Shichida, Y., Lanyi, J. K., & Maeda, A. (1992) *J. Biol. Chem. 267*, 20782–20786.
Schulten, K., Schulten, Z., & Tavan, P. (1984) in *Information and Energy Transduction in Biological Membranes* (Bolis, A., Helmreich, H., & Passow, H., Eds.) pp 113–131, H. Alan R. Liss, Inc., New York.
Stern, L. J., & Khorana, H. G. (1989) *J. Biol. Chem. 264*, 14202–14208.
Subramaniam, S., Marti, T., & Khorana, H. G. (1990) *Proc. Natl. Acad. Sci. U.S.A. 87*, 1013–1017.
Thorgeirsson, T. E., Milder, S. J., Miercke, L. J. W., Betlach, M. C., Shand, R. F., Stroud, R. M., & Kliger, D. S. (1991) *Biochemistry 30*, 9133–9142.
Tittor, J., Soell, C., Oesterhelt, D., Butt, H.-J., & Bamberg, E. (1989) *EMBO J. 8*, 3477–3482.
Váró, G., & Lanyi, J. K. (1989) *Biophys. J. 56*, 1143–1151.
Váró, G., & Lanyi, J. K. (1990a) *Biochemistry 29*, 2241–2250.
Váró, G., & Lanyi, J. K. (1990b) *Biochemistry 29*, 6858–6865.
Váró, G., & Lanyi, J. K. (1991a) *Biochemistry 30*, 5016–5022.
Váró, G., & Lanyi, J. K. (1991b) *Biophys. J. 59*, 313–322.
Váró, G., & Lanyi, J. K. (1991c) *Biochemistry 30*, 5008–5015.
Zimányi, L., Keszthelyi, L., & Lanyi, J. K. (1989) *Biochemistry 28*, 5165–5172.
Zimányi, L., Cao, Y., Chang, M., Ni, B., Needleman, R., & Lanyi, J. K. (1992a) *Photochem. Photobiol. 56*, 1049–1055.
Zimányi, L., Váró, G., Chang, M., Ni, B., Needleman, R., & Lanyi, J. K. (1992b) *Biochemistry 31*, 8535–8543.